DOI: 10.1021/ic900657w

Inorganic Chemistry
Article

Cap for Copper(I) Ions! Metallosupramolecular Solid and Solution State Structures on the Basis of the Dynamic Tetrahedral $[Cu(phenAr_2)(py)_2]^+$ Motif

Michael Schmittel,*,† Bice He,† Jian Fan,† Jan W. Bats,‡ Marianne Engeser,§ Marc Schlosser,∥ and Hans-Jörg Deiseroth∥

†*Center of Micro and Nanochemistry and Engineering, Organische Chemie I, Universität Siegen, Adolf-Reichwein-Strasse 2, D-57068 Siegen, Germany,* ‡*Institute für Organische Chemie und Chemische Biologie, Johann Wolfgang Goethe-Universität, Max-von-Laue-Strasse 7, D-60438 Frankfurt am Main, Germany,* §*Kekulé-Institut für Organische Chemie und Biochemie der Universität Bonn, Gerhard-Domagk-Strasse 1, 53121 Bonn, Germany, and* ∥*Anorganische Chemie I, Universität Siegen, Adolf-Reichwein-Strasse 2, D-57068 Siegen, Germany*

Received March 24, 2009

The tetrahedral $[Cu(phenAr_2)(py)_2]^+$ coordination motif (phen = 1,10-phenanthroline; py = pyridine) conceived on the basis of the HETPYP concept (*het*eroleptic *py*ridyl and *p*henanthroline metal complexes) is a versatile dynamic unit for constructing various heteroleptic metallosupramolecular *pseudo*-1D, 2D, and 3D structures, both in solution and the solid state. The 2,9-diaryl substituted phenanthroline ($phenAr_2$) serves as a capping ligand for copper(I) ions, as its bulky nature prevents formation of the homoleptic complex $[Cu(phenAr_2)_2]^+$. Combination of the dynamic and concave metal ligand building block $[Cu(phenAr_2)]^+$ with various pyridine (py) ligands, such as bi-, tri-, and tetrapyridines, opened the way to infinite 1D helicates, 2D networks, and discrete 3D hexanuclear cages, whereas spatial integration of both $phenAr_2$ and py units into a single ligand resulted in the formation of a Borromean-ring-type hexanuclear cage.

Introduction

The huge success of Fujita's and Stang's coordination concepts using end-capped square-planar palladium and platinum units has been documented over the last 15 years in countless reports.[1,2] A variety of ligands, such as pyridines, alkynes, and nitriles, was shown to dynamically bind to the end-capped Pd and Pt units (Scheme 1), allowing to set up various spectacular metallosupramolecular structures, such as squares, cages, and so forth.[1] A possible limitation of the above concepts, though, is that the kinetically inert end-cap is not involved in the dynamic interplay. Herein, we would like to introduce an extension of the above concepts, in which the metal center, now a copper(I) ion, is setting up a tetrahedral coordination scenario with one phenanthroline and two pyridines serving as ligands (Scheme 1). Most distinctly, the phenanthroline end-cap is not bound in a kinetically inert fashion to the copper center, which should allow reduction of the activation barriers in intricate multitopic aggregate formation, in particular if one starts out from oligophenanthrolines serving as an end-cap at several metal centers. Herein, we would like to demonstrate that despite the weak and dynamic binding of three ligands at a copper center, the heteroleptic $[Cu(phenAr_2)(py)_2]^+$ scenario is maintained in all solution and solid state structures.

Because of its strong binding to various metal ions, the parent 1,10-phenanthroline (phen) ligand has become a versatile building block for a large number of supramolecular self-assembled structures.[3] Our group has contributed to this field by developing labile heteroleptic combinations using the concave $[M(phenAr_2)]^{n+}$ fragment as a starting point.[4] Because of the steric shielding of the metal fragment by appropriately sized aryl groups Ar (for example,

*To whom correspondence should be addressed. E-mail: schmittel@chemie.uni-siegen.de.

(1) (a) Fujita, M.; Yazaki, J.; Ogura, K. *J. Am. Chem. Soc.* **1990**, *112*, 5645–5647. (b) Fujita, M.; Tominaga, M.; Hori, A.; Therrien, B. *Acc. Chem. Res.* **2005**, *38*, 371–380.

(2) (a) Stang, P. J.; Cao, D. H. *J. Am. Chem. Soc.* **1994**, *116*, 4981–4982. (b) Seidel, S. R.; Stang, P. J. *Acc. Chem. Res.* **2002**, *35*, 972–983.

(3) (a) Dwyer, F. P.; Gyarfas, E. C.; Rogers, W. P.; Koch, J. H. *Nature* **1952**, *170*, 190–191. (b) Armaroli, N.; Balzani, V.; Barigelletti, F.; De Cola, L.; Sauvage, J.-P.; Hemmert, C. *J. Am. Chem. Soc.* **1991**, *113*, 4033–4035. (c) Payer, D.; Rauschenbach, S.; Malinowski, N.; Konuma, M.; Virojanadara, C.; Starke, U.; Dietrich-Buchecker, C.; Collin, J.-P.; Sauvage, J.-P.; Lin, N.; Kern, K. *J. Am. Chem. Soc.* **2007**, *129*, 15662–15667. (d) Prikhod'ko, A. I.; Durola, F.; Sauvage, J.-P. *J. Am. Chem. Soc.* **2008**, *130*, 448–449. (e) Coronado, E.; Galan-Mascaros, J. R.; Gaviña, P.; Martí-Gastaldo, C.; Romero, F. M.; Tatay, S. *Inorg. Chem.* **2008**, *47*, 5197–5203.

(4) (a) Schmittel, M.; Ganz, A. *Chem. Commun.* **1997**, 999–1000. (b) Schmittel, M.; Lüning, U.; Meder, M.; Ganz, A.; Michel, C.; Herderich, M. *Heterocycl. Commun.* **1997**, *3*, 493–498. (c) Schmittel, M.; Michel, C.; Liu, S.-X.; Schildbach, D.; Fenske, D. *Eur. J. Inorg. Chem.* **2001**, 1155–1166.

Published on Web 08/04/2009

Scheme 1. Caps Used for Metal Ion Complexes

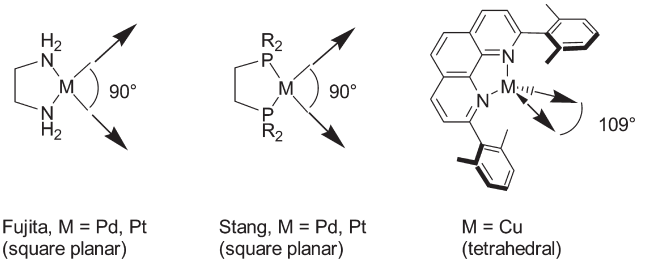

Ar = 2,4,6-trimethylphenyl) in phenAr_2, the $[M(phenAr_2)]^{n+}$ unit is arrested against formation of a bishomoleptic complex $[M(phenAr_2)_2]^{n+}$ even if the phenAr_2 is present in large excess over the metal ion. Such a particular setting allows the combination of the $[M(phenAr_2)]^{n+}$ fragment with a second, but sterically undemanding phenanthroline to afford $[M(phenAr_2)(phen)]^{n+}$ (M^{n+} = Cu^+, Ag^+, Zn^{2+})[5] or with a sterically unpretentious terpyridine (terpy) to yield $[M(phenAr_2)(terpy)]^{n+}$ combinations (M^{n+} = Cu^+, Hg^{2+}, Zn^{2+}).[6] Two main effects aid heteroleptic aggregation in the above-mentioned complexes: (i) maximum site occupancy[7] and (ii) a strong donor−acceptor interaction between the aryl groups Ar of phenAr_2 and the second metal bound ligand (a phenanthroline in the HETPHEN concept, and a terpyridine in the HETTAP approach).

The quantitative formation of heteroleptic mononuclear complexes along the HETPHEN (HETeroleptic BisPHENanthroline Complexes)[4,5] or HETTAP (HETeroleptic Terpyridine And Phenanthroline Complexes)[6] concept found ample use in the quantitative preparation of polynuclear supramolecular frameworks, such as nanosized ladders, grids, racks, dumbbells, and other topologies.[4−6] The combination of several bi- or tridentate ligands at dynamically binding metal ion centers in supramolecular assemblies, however, operates at the cost of a slow kinetics. The latter issue becomes more and more virulent the larger and more intricate the supramolecular framework.[6b,6c,8] It thus seemed necessary to find the right balance between thermodynamics and kinetics to realize a facilitated access to kinetically demanding nanostructures. Unlike phen or terpy, non-chelating monodentate pyridine ligands provide much weaker binding with metal ions, but because of their increased kinetics

Scheme 2. Dynamic Heteroleptic Complex Motifs

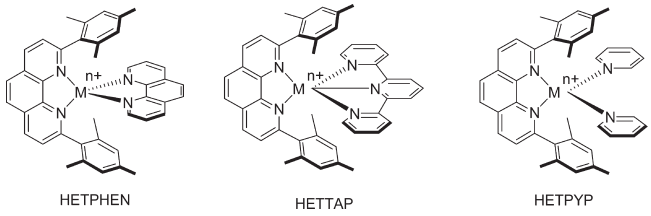

in combination with a flexible binding geometry, they have an enormous potential for exciting nanostructures,[1b,2b,9] in particular in combination with poly(pyridine) building blocks (4,4′-bipyridine[10] and 1,3,5-tripyridyltriazine[1d]).

Until now, metal complexes $[M(py)_2L_m]^{n+}$ with pyridine (py) as ligand have been investigated extensively for square-planar coordinated metal ions, such as palladium and platinum,[1,2,11] whereas metal ions with a tetrahedral coordination environment, as copper(I) ions, have been reported amazingly seldom.[12] Therefore, as an extension of the HETPHEN concept,[4] we seeked to explore the HETPYP approach (HETeroleptic PYridyl and Phenanthroline metal complexes), which brings together pyridine and phenanthroline ligands at a tetrahedrally coordinating metal center to form dynamic $[M(phenAr_2)(py)_2]^{n+}$ complexes (Scheme 2, right). While this method should work equally well for Cu^+, Ag^+, and Zn^{2+}, we have concentrated our first efforts on copper(I) ions. As a prerequisite, we used a phenanthroline that is shielded by large 2,9-aryl groups (phenAr_2) in a way that its complexation process in absence of pyridine ligands will arrest at the $[Cu(phenAr_2)]^+$ exposing two vacant coordination sites (usually occupied by loosely bound solvent molecules). In a way, the $[Cu(phenAr_2)]^+$ unit is a capped metal center analogous to $M(Me_2N\text{-}X\text{-}NMe_2)$ or $M(Ph_2P\text{-}X\text{-}PPh_2)$ with M = Pd, Pt. We will demonstrate that such an approach opens structural options for simple and intricate complexes that are complementary to the well-known palladium and platinum chemistry.

All ligands used in this report are depicted in Scheme 3. 4,4′-Bipyridine (**BP**) and the tetrakispyridine **TPP** were purchased and used as supplied without further purification. Phenanthrolines **Phen1**[6a] and **Phen2**[6a] as well as tripyridine **TP**[13] were prepared according to literature procedures. **Phen3** was prepared as described in the Supporting Information.

(5) (a) Schmittel, M.; Ganz, A.; Fenske, D. *Org. Lett.* **2002**, *4*, 2289–2292. (b) Schmittel, M.; Ammon, H.; Kalsani, V.; Wiegrefe, A.; Michel, C. *Chem. Commun.* **2002**, 2566–2567. (c) Schmittel, M.; Kalsani, V.; Fenske, D.; Wiegrefe, A. *Chem. Commun.* **2004**, 490–491. (d) Schmittel, M.; Kishore, R. S. K. *Org. Lett.* **2004**, *6*, 1923–1926. (d) Schmittel, M.; Kalsani, V.; Michel, C.; Mal, P.; Ammon, H.; Jäckel, F.; Rabe, J. P. *Chem.—Eur. J.* **2007**, *13*, 6223–6237.

(6) (a) Schmittel, M.; Kalsani, V.; Kishore, R. S. K.; Cölfen, H.; Bats, J. W. *J. Am. Chem. Soc.* **2005**, *127*, 11544–11545. (b) Schmittel, M.; He, B.; Mal, P. *Org. Lett.* **2008**, *10*, 2513–2516. (c) Schmittel, M.; He, B. *Chem. Commun.* **2008**, 4723–4725.

(7) (a) Baxter, P. N. W.; Lehn, J.-M.; Kneisel, B. O.; Baum, G.; Fenske, D. *Chem.—Eur. J.* **1999**, *5*, 113–120. (b) Garcia, A. M.; Bassani, D. M.; Lehn, J.-M.; Baum, G.; Fenske, D. *Chem.—Eur. J.* **1999**, *5*, 1234–1238.

(8) (c) Al-Rasbi, N. K.; Tidmarsh, I. S.; Argent, S. P.; Adams, H.; Harding, L. P.; Ward, M. D. *J. Am. Chem. Soc.* **2008**, *130*, 11641–11649.

(9) (a) Takeda, N.; Umemoto, K.; Yamakuchi, K.; Fujita, M. *Nature* **1999**, *398*, 794–796. (b) Olenyuk, B.; Whiteford, J. A.; Fechtenkötter, A.; Stang, P. J. *Nature* **1999**, *398*, 796–799. (c) Kuehl, C. J.; Yamamoto, T.; Seidel, S. R.; Stang, P. J. *Org. Lett.* **2002**, *4*, 913–915. (d) Yoshizawa, M.; Nakagawa, J.; Kumazawa, K.; Nagao, M.; Kawano, M.; Ozeki, T.; Fujita, M. *Angew. Chem., Int. Ed.* **2005**, *44*, 1810–1813. (e) Tashiro, S.; Kobayashi, M.; Fujita, M. *J. Am. Chem. Soc.* **2006**, *128*, 9280–9281. (f) Sato, S.; Lida, J.; Suzuki, K.; Kawano, M.; Ozeki, T.; Fujita, M. *Science* **2006**, *313*, 1273–1276.

(10) Rannulu, N. S.; Rodgers, M. T. *J. Phys. Chem. A* **2007**, *111*, 3465–3479.

(11) (a) Fujita, M.; Yazaki, J.; Ogura, K. *Chem. Lett.* **1991**, 1031–1032. (b) Drain, C. M.; Lehn, J.-M. *J. Chem. Soc. Chem. Commun.* **1994**, 2313–2315. (c) Olenyuk, B.; Whiteford, J. A.; Stang, P. J. *J. Am. Chem. Soc.* **1996**, *118*, 8221–8230. (d) Stang, P. J.; Fan, J.; Olenyuk, B. *Chem. Commun.* **1997**, 1453–1454. (e) Stang, P. J.; Cao, D. H.; Chen, K.; Gray, G. M.; Muddiman, D. C.; Smith, R. D. *J. Am. Chem. Soc.* **1997**, *119*, 5163–5168. (f) Lahav, M.; Gabai, R.; Shipway, A. N.; Willner, I. *Chem. Commun.* **1999**, 1937–1938. (g) Fan, J.; Whiteford, J. A.; Olenyuk, B.; Levin, M. D.; Stang, P. J.; Fleischer, E. B. *J. Am. Chem. Soc.* **1999**, *121*, 2741–2752. (h) Würthner, F.; Sautter, A. *Chem. Commun.* **2000**, 445–446. (i) Würthner, F.; Sautter, A. *Org. Biomol. Chem.* **2003**, *1*, 240–243. (j) Kaletaş, B. K.; Dobrawa, R.; Sautter, A.; Würthner, F.; Zimine, M.; De Cola, L.; Williams, R. M. *J. Phys. Chem. A* **2004**, *108*, 1900–1909.

(12) (a) Blake, A. J.; Hill, S. J.; Hubberstey, P.; Li, W.-S. *J. Chem. Soc., Dalton Trans.* **1998**, 909–915. (b) Blake, A. J.; Hubberstey, P.; Li, W.-S.; Quinlan, D. J.; Russell, C. E.; Sampson, C. L. *J. Chem. Soc., Dalton Trans.* **1999**, 4261–4268.

(13) Asselberghs, I.; Hennrich, G.; Clays, K. *J. Phys. Chem. A* **2006**, *110*, 6271–6275.

Scheme 3. Ligands Used in the Present Study

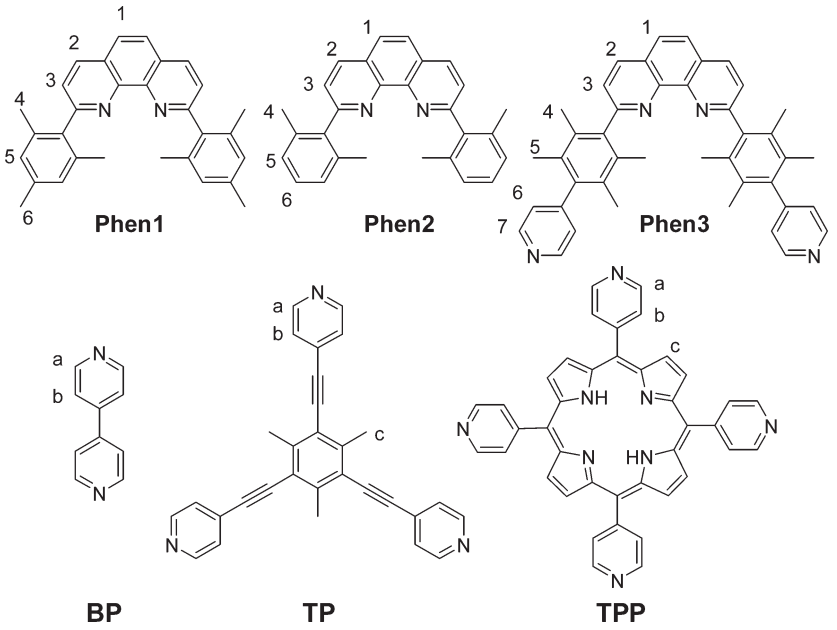

Results and Discussion

Pseudo-1D Supramolecular Helicates. Our first idea aimed at using the heteroleptic complex motif $[Cu(phenAr_2)(py)_2]^+$ to construct a supramolecular polygon, which we expected to form from **Phen1** and **BP** (1:1) in the presence of 1 equiv of $[Cu(MeCN)_4]PF_6$ despite some angular strain at the tetrahedrally coordinated metal center in dichloromethane. When we dissolved the corresponding product in dichloromethane-d_2, the ^{1}H NMR spectrum showed the expected set of sharp signals indicative of the formation of a single species. Notably, the chemical shifts of both protons of **BP** were dramatically upfield shifted from 8.71 to 7.75 and from 7.55 ppm to 7.39 ppm because of the **BP** protons being positioned in the shielding region of mesityl groups of **Phen1**. Because of the identical shielding of both pyridine rings in **BP**, one is led to postulate the formation of polygons or an infinite linear arrangement. ESI FT-ICR MS spectra of the solution, however, showed only signals representing small fragments such as $[Cu(\mathbf{Phen1})(\mathbf{BP})]^+$ and $[Cu_2(\mathbf{Phen1})_2(\mathbf{BP})(PF_6)]^+$, clearly witnessing a weak coordination bond in $[Cu(phenAr_2)]^+\cdots$py aggregates, which as a consequence do not fully survive gas phase ionization. Unfortunately, although single crystals of rather big size and good shape were obtained by different methods and in different solvents, all crystals proved to be unstable during diffraction measurements. Even at low temperature, the crystal broke up easily, and even wrapping up in oil or locating in the original solvent would not prolong its stability.

Importantly, changing the ligand **Phen1** to **Phen2** caused a big difference. When **Phen2** and **BP** (1:1) were combined with 1 equiv of $[Cu(MeCN)_4]PF_6$ in dichloromethane-d_2, small crystals precipitated out in less than 10 min, precluding the measurement of the ^{1}H NMR spectrum. This finding already suggested that bigger aggregates, possibly oligomers or polymers, were formed in solution. Upon addition of 5% (v/v) of acetonitrile-d_3 to the precipitated complex (in dichloromethane), a clear solution was obtained immediately. A ^{1}H NMR spectrum of this solution exhibited no shifts for the protons different from those of the free constituents, suggesting that acetonitrile had eventually broken up the [(phenAr_2)-Cu(I)]---py coordination releasing free **BP**. An ESI FT-ICR MS spectrum of this solution surprisingly revealed not only signals of small fragments, such as $[Cu(\mathbf{Phen2})(\mathbf{BP})]^+$ and $[Cu_2(\mathbf{Phen2})_2(\mathbf{BP})(PF_6)]^+$, but also of larger aggregates, like $[Cu_3(\mathbf{Phen2})_3(\mathbf{BP})_2(PF_6)_2]^+$. Combining the evidence from ^{1}H NMR and the ESI FT-ICR MS, it seems plausible that the addition of acetonitrile reduced the [(phenAr_2)Cu(I)]---py coordination in solution by increasing the dynamic exchange at the metal center. However, under the vacuum conditions of the mass spectrometry experiment, that is, after removal of acetonitrile, a substantial fraction of [(phenAr_2)Cu(I)]---py coordinated fragments showed up as demonstrated by the ESI FT-ICR MS results.

Fortunately, single crystals suitable for X-ray analysis were obtained by slow evaporation of acetonitrile from a 1,2-dichlorobenzene/acetonitrile solution of **Phen2**, **BP**, and $[Cu(MeCN)_4]PF_6$ (1:1:1). The resultant product is denoted as complex **2** in the following. As depicted in Figure 1, each copper(I) ion, as expected, is tetrahedrally coordinated by two nitrogen atoms from one phenanthroline and two nitrogen atoms from two bipyridines. Each bipyridine **BP** connects two copper-phenanthroline units, which leads to the formation of a one-dimensional (1D) structure. Furthermore, the crystal structure of complex **2** displays right-handed and left-handed helicates with a pitch of 27.6 Å, rather than zigzag chains[12a] as reported by Blake et al., who used a simple unsubstituted phenanthroline in combination with **BP**. Each helicate propagates along the *c* axis, generating a prismatic cavity with an opening of about 8.7 × 8.7 Å^2. In complex **2**, any left-handed helicate is surrounded by four right-handed helicates with interpenetration of their grooves, and vice versa (Figure 1, left). The PF_6^- anions are located in between two Cu(I) coordination centers from two

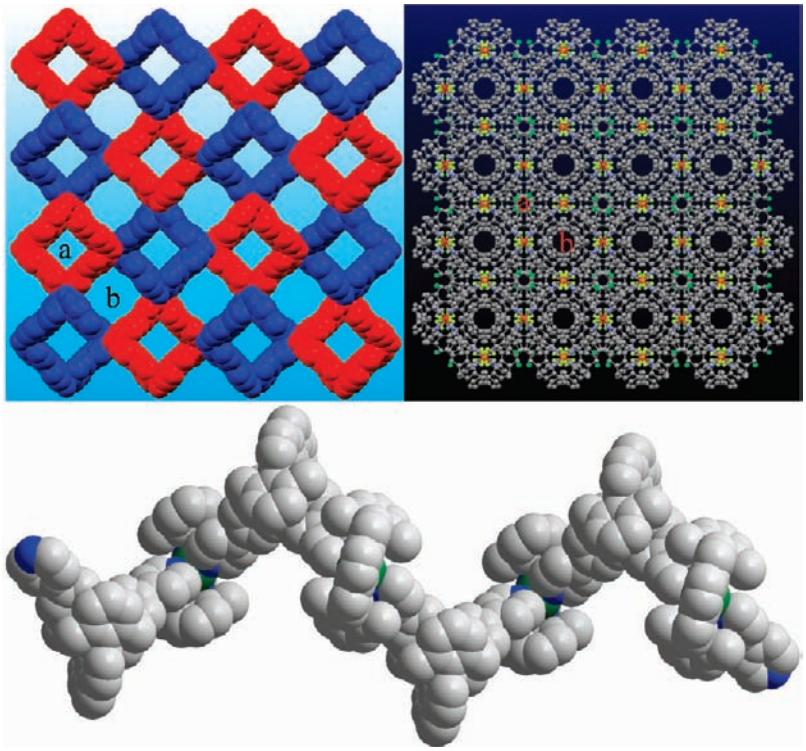

Figure 1. (Top left) Top view of the crystal packing of complex **2** with left- and right-handed helicates in red and blue, respectively. The capping ligand **Phen2**, solvate molecules, anions, and hydrogen atoms were omitted for clarity. (Top right) Top view of crystal packing of complex **2** with hydrogen atoms omitted for clarity. Carbon, gray; Nitrogen, blue; Copper, red (hidden); Phosphorus, Orange; Fluorine, yellow; Chlorine, green. (Bottom) Side view of the X-ray structure showing a right-handed helix of complex **2**. Carbon, gray; Nitrogen, blue; Copper, green. Solvate molecules, anions and hydrogen were omitted for clarity.

adjacent helicates. Related PF_6^- anions and Cu(I) cations are exactly located on a straight line (Figure 1, right). All 1,2-dichlorobenzene solvate molecules are located inside channels **a** formed by a single helicate, while channels **b** formed by four adjacent helicates remain empty.

From the data it seems that both in solution and in the solid state the combination of **Phen2**, **BP**, and $[Cu(MeCN)_4]PF_6$ (1:1:1) leads to coordination polymers $[Cu(\mathbf{Phen2})(\mathbf{BP})]_n^{n+}$. The high lability and weak Cu--py coordination does not allow to differentiate between linear or cyclic oligomers in solution, for which there are some precedents with copper in oxidation state 2+.[14]

From the above results it becomes clear that the $[Cu(phenAr_2)(py)_2]^+$ is a continual motif with **Phen1**/**Phen2** and **BP** recurring both in the solid state and solution, with the restriction that ^{1}H NMR and ESI FT-ICR MS do not allow a full structural identification in the latter medium.

From a Truncated Tetrahedron to a Broken Honeycomb Network. Encouraged by the successful application of the $[M(phenAr_2)(py)_2]^{n+}$ motif as illustrated by the formation of complex **2**, we seeked to replace bipyridine **BP** by tripyridine **TP**. With py in $[M(phenAr_2)(py)_2]^{n+}$ being represented by **TP** we envisioned that the smallest supramolecular entity formed at lowest entropic costs and correct maximum site occupancy should be the hexanuclear $[Cu_6(\mathbf{Phen1})_6(\mathbf{TP})_4]^{6+}$ cage. Indeed, combination of **Phen1**, **TP** and $[Cu(MeCN)_4]PF_6$ (6:4:6) in dichloromethane resulted in the formation of the Fujita type of truncated tetrahedral cage[9a,15] **3c** (**c** for cage, Figure 2) as demonstrated by solution characterization techniques, while crystallization led to another structure, the broken honeycomb network, herein denoted as **3n** (see Figure 4, n for network).

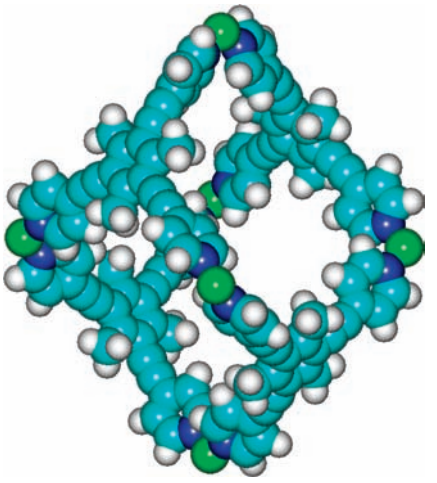

Figure 2. HyperChem structure of cage **3c**. Carbon, cyan; Nitrogen, blue; Copper, green; Hydrogen, white. The ligand **Phen1** bound to each of the six copper centers was omitted for clarity.

Undoubtedly, the solution structure **3c** is different from the solid state structure **3n** on the basis of all data. For example, the ^{1}H NMR of **3c**, exhibiting a single set of

(14) Liu, G.-F.; Ren, Z.-G.; Li, H.-X.; Chen, Y.; Li, Q.-H.; Zhang, Y.; Lang, J.-P. *Eur. J. Inorg. Chem.* **2007**, 5511–5522. Al-Rasbi, N. K.; Adams, H.; Harding, L. P.; Ward, M. D. *Eur. J. Inorg. Chem.* **2007**, 4770–4780.

(15) Abrahams, B. F.; Batten, S. R.; Hamit, H.; Hoskins, B. F.; Robson, R. *Angew. Chem., Int. Ed. Engl.* **1996**, *35*, 1690–1692.

signals, is characterized by large upfield shifts of the pyridine protons of **TP** to 7.65 and 7.28 ppm! Equally, the DOSY NMR spectrum confirmed the formation of a single product (see Supporting Information). Though the binding in complex **3c** was not strong enough to survive standard ESI-MS conditions, the ESI FT-ICR MS analysis provided clear clues for the existence of the hexanuclear cage **3c** in solution by showing the corresponding signals: m/z 2577.2 Da for $[Cu_6(\mathbf{Phen1})_6(\mathbf{TP})_4)(PF_6)_4]^{2+}$) and fragments thereof (2264.8 Da, $[Cu_5(\mathbf{Phen1})_5(\mathbf{TP})_4)(PF_6)_3]^{2+}$; 2053.2 Da, $[Cu_5(\mathbf{Phen1})_5(\mathbf{TP})_3)(PF_6)_3]^{2+}$; 1951.7 Da, $[Cu_4(\mathbf{Phen1})_4(\mathbf{TP})_4)(PF_6)_2]^{2+}$; 1740.1 Da, $[Cu_4(\mathbf{Phen1})_4(\mathbf{TP})_3)(PF_6)_2]^{2+}$; and so on).

After slow vapor diffusion of diethylether into the solution of complex **3c** in dichloromethane, red needle-shaped crystals were obtained, but they were too small to be measured. After dissolving the complex in a mixture of acetonitrile and dichlorobenzene (10:1) in a small vial and after allowing slow evaporation of acetonitrile to occur, big crystals in form of red rods were obtained that proved to be insoluble in dichloromethane. As already mentioned above, the solid state structure of complex **3n** (Figure 3) showed a two-dimensional (2D) honeycomb arrangement rather then a truncated tetrahedron as postulated for **3c**.

The X-ray analysis, unfortunately of low quality, revealed a 2D broken honeycomb network with huge pores, each of which exhibited a size of about 780 Å^2. Every single pore contains six **TP** ligands and six Cu-Phen species (Figure 3), and actually represents a combination of three adjacent hexagons of a classical honeycomb (Figure 4, left). The 2D sheets do not overlap with each other in a perfect superimposition, which would result in a pore size of the channels of 780 Å^2. Rather, the 2D sheets are shifted relative to each other by about 1.0 nm (from ideal superimposition), thereby forming hexagonal channels with a smaller opening of about 260 Å^2 (Figure 4, right). All solvate molecules and anions are located in those channels. Since in the solution state, the combination of **Phen1**, **TP**, and $[Cu(MeCN)_4]PF_6$ (6:4:6) resulted in a discrete cage as postulated on the basis of the ^{1}H NMR, DOSY, and FT-ICR MS, the different solid state structure is presumably due to solid state effects resulting from crystal packing, solvate effects and so on.[16] Notably, once again the $[Cu(phenAr_2)(py)_2]^+$ unit proved to be a continual motif in both solution and the solid state, now with **TP** as a pyridine ligand.

Porphyrinic Network. To further challenge the exclusive formation of the $[Cu(phenAr_2)(py)_2]^+$ unit with a tetrapyridine ligand, the reaction of the capping phenanthroline **Phen1** and copper(I) ions with the tetrapyridine **TPP** was probed. This combination is even more interesting, as the reaction of copper(II)-filled **TPP** with $[Cu(MeCN)_4]X$ has been reported to lead to three-dimensional (3D) networks with large channels.[17] To probe the self-assembly along the HETPYP approach, the reaction of **Phen1**, Zn-**TPP** (or Cu-**TPP**), and $[Cu(MeCN)_4]PF_6$ (2:1:2) in various solvents system was explored. However, because of the extremely low solubility of Zn- and Cu-**TPP**, all our attempts failed. Since the low solubility of metal porphyrins is a consequence of self-aggregation via metal--pyridine association,[17] it was envisioned to start out from the free base porphyrin **TPP** with its increased solubility instead. If self-assembly along the HETPYP concept were faster than metal insertion into **TPP** to yield Cu-**TPP**, a kinetically controlled solid state assembly could potentially form. As the transformation of **TPP** to Cu-**TPP** in a reaction system containing $[Cu(MeCN)_4]PF_6$ cannot be prevented with time, we have to make sure that 100% of **TPP** will be converted to Cu-**TPP** by adding some extra amount of $[Cu(MeCN)_4]PF_6$. On the basis of these considerations, a mixture of **Phen1**, **TPP**, and $[Cu(MeCN)_4]PF_6$ (2:1:3) in dichlorobenzene/acetonitrile (8:2) was heated to reflux for 2 h. After cooling to room temperature and slow evaporation of acetonitrile, single crystals of complex **4** suitable for X-ray diffraction measurement were obtained.

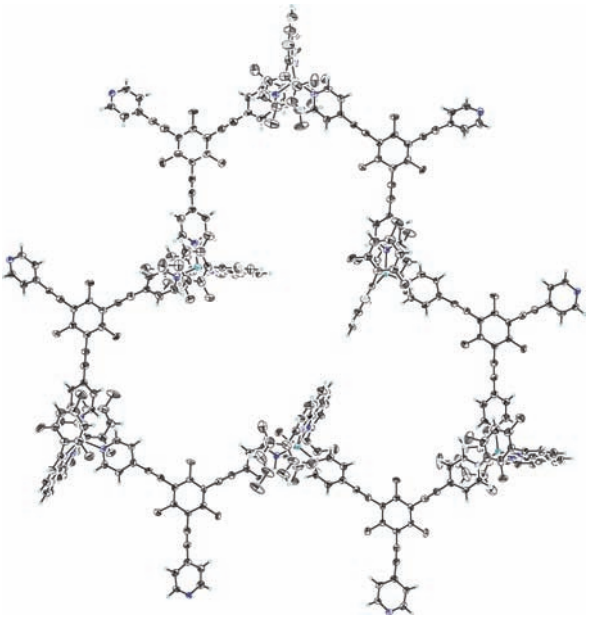

Figure 3. Top view of crystal structure of complex **3n**. Solvate molecules were omitted for clarity.

Though the crystal quality of **4** was not very high, a structure determination was still possible. From the X-ray structure shown in Figure 5, it becomes apparent that each porphyrin unit is now filled with a copper ion. While in complex **2**, the Cu-Phen motifs are connected by a bifurcate ligand (**BP**) to form the 1D helicate, in complex **4**, the Cu-Phen motifs are linked by a tetrafurcate ligand (Cu-**TPP**) to generate a 2D structure. Each copper(I) is tetrahedrally coordinated as observed in **4**. The planes of two adjacent porphyrin units around one copper(I) center are perpendicular to each other (Figure 6), resulting in a puckered layer structure. Any of the Cu-**TPP** ligand connects to four Cu-**TPP** units and every four Cu-**TPP** units form a big cavity with a size of about 13.4 × 24.1 Å^2 (estimated by the distance of the diagonal copper ions within one cavity), where anions, solvate molecules, and the bulky groups at 2,9-position of **Phen1** are accommodated. The phenanthroline ligand **Phen1** acts like a scissor cutting the Robson's 3D networks into 2D sheets by replacing the two pyridyl units delivered by two Cu-**TPP** ligands (as in solution) by a

(16) Pentecost, C. D.; Chichak, K. S.; Peters, A. J.; Cave, G. W. V.; Cantrill, S. J.; Stoddart, J. F. *Angew. Chem., Int. Ed.* **2007**, *46*, 218–222.
(17) Abrahams, B. F.; Hoskins, B. F.; Michail, D. M.; Robson, R. *Nature* **1994**, *369*, 727–729.

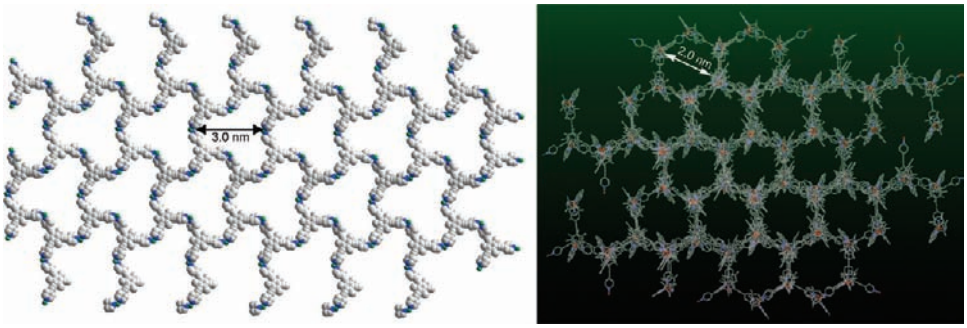

Figure 4. X-ray structure of complex **3n**. Left: space filling presentation of a single layer of the tripyridine/Cu^{+} skeleton of **3n** (phenanthrolines are omitted for clarity). Right: stick presentation of the multilayer network of **3n** (solvate molecules, anions, and hydrogen were omitted for clarity).

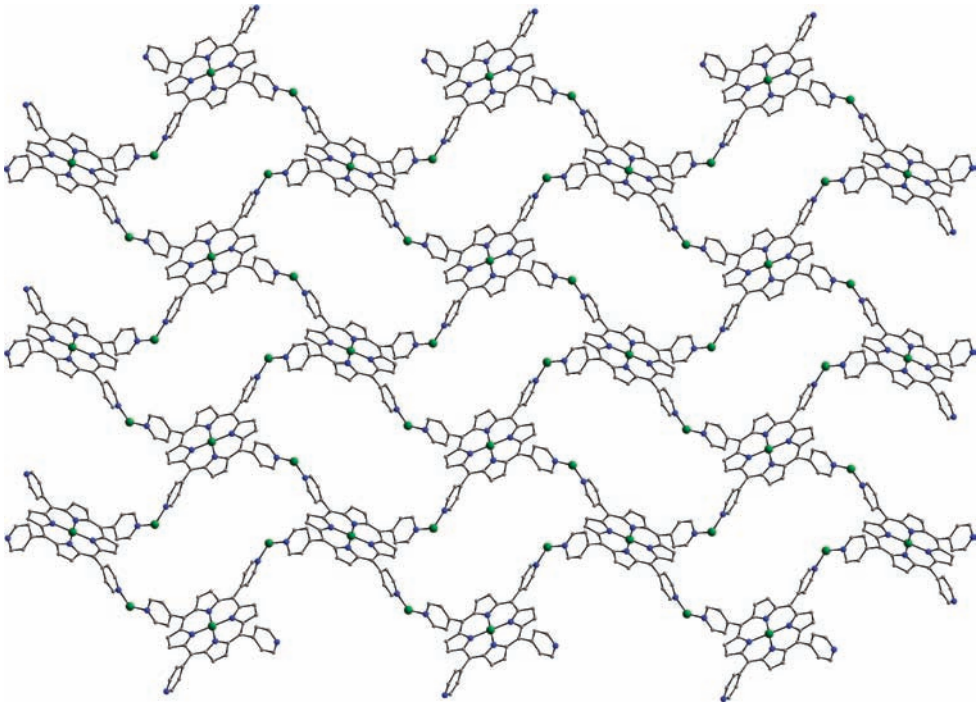

Figure 5. X-ray structure of complex **4**. Carbon, gray; Nitrogen, blue; Copper, green. Ligand **Phen1**, solvate molecules, anions, and hydrogen atoms were omitted for clarity.

single **Phen1** ligand. The N(Py)−Cu-N(Py) angle is 104.2°.

Hexanuclear Cage (Borromean-Ring-Type Structure). All experiments delineated above have shown a high fidelity in the formation of the $[Cu(phenAr_2)(py)_2]^+$ motif, in both solution and the solid state. For testing a sterically congested self-assembly process, we decided to spatially integrate the $phenAr_2$ and the py coordination motifs into a single ligand, as realized in **Phen3**. Reaction of **Phen3** and $[Cu(MeCN)_4]PF_6$ (1:1) afforded smoothly the hexanuclear cage **5** (Figure 7), whose smaller analogue had been reported earlier by Champness et al., though without control of heteroleptic aggregation.[18] Hence, while the $phenAr_2$ unit in **Phen3** ascertains heteroleptic aggregation at the copper(I) center, this is no *conditio sine qua non* for systems with a spatial integration of the phenanthroline and pyridine unit.

Cage **5** was fully characterized by ordinary ESI-MS with the spectrum showing a clear set of signals corresponding to the expected cage with a charge range from 3+ to 6+ (see Supporting Information). The facile ESI-MS characterization of cage **5** indicated that because of the mutual binding of in total six **Phen3**, all parts are held together more tightly than in **3c**. The ^1H NMR spectrum of cage **5** showed a clear single set of signals with upfield shifts for the py 7-H protons. Besides, the DOSY spectrum of cage **5** confirmed the formation of a single product by showing a single set of signals (see Supporting Information).

From the X-ray structure, depicted in Figure 7, cage **5** has the structure of Borromean rings.[19] In each case, two ligands **Phen3** and two Cu(I) metal ions form one rhombus (or ring), and the resulting three rhombuses are

(18) Dolomanov, O. V.; Blake, A. J.; Champness, N. R.; Schröder, M.; Wilson, C. *Chem. Commun.* **2003**, 682–683.

(19) (a) Chichak, K. S.; Cantrill, S. J.; Pease, A. R.; Chiu, S.-H.; Cave, G. W. V.; Atwood, J. L.; Stoddart, J. F. *Science* **2004**, *304*, 1308–1312. (b) Cantrill, S. J.; Chichak, K. S.; Peters, A. J.; Stoddart, J. F. *Acc. Chem. Res.* **2005**, *38*, 1–9.

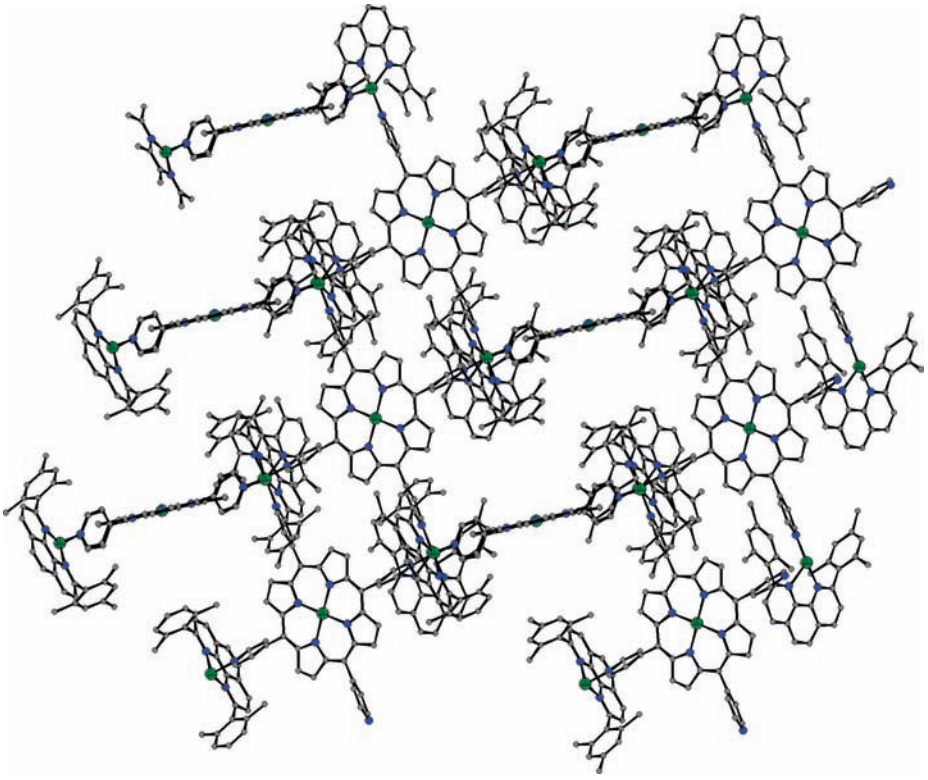

Figure 6. X-ray structure of complex **4**. Carbon, gray; Nitrogen, blue; Copper, green. Solvate molecules, anions, and hydrogen atoms were omitted for clarity.

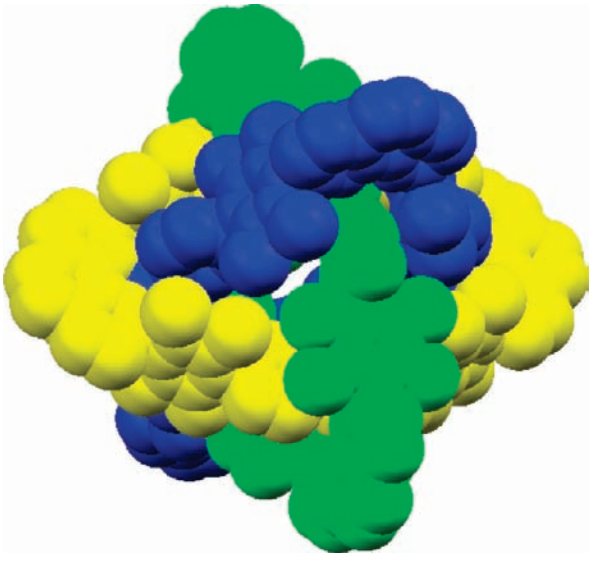

Figure 7. X-ray structure of cage **5**. Solvate molecules, anions, and hydrogen were omitted for clarity.

interlocked with each other via copper(I) coordination centers, at which the phenanthroline and pyridyl units act as *endo* and *exo* binding ligands, respectively. Since the two arms of **Phen3** comprise an angle of 60°, the angle of $N_{py}-Cu-N_{py}$ should be 120° according to the geometry of a rhombus. This is in good agreement with the experimental value of 116.2° indicating that each arm is only distorted from the ideal angle by about 1.9°. The cavity of cage **5** is around 610 $Å^3$ in size calculated from the positions of the Cu(I) coordination centers. Both ^{31}P and ^{19}F NMR spectra show two sets of signals with a ratio around 5:1, suggesting that the cavity accommodates one out of the six PF_6^- anions as a guest. In contrast, the cavity of the truncated tetrahedral cage **3c** is much larger with 2700 $Å^3$ in volume (calculated from HyperChem structure, Figure 2). Since the cavity of **3c** in addition has rather large portals, anions may go into and out easily. Indeed, for **3c** ^{31}P and ^{19}F NMR studies showed only one set of signals.

Conclusion

Our concept to use 2,9-aryl substituted phenanthrolines to dynamically cap copper(I) ions and to set up a tetrahedral $[Cu(phenAr_2)(py)_2]^+$ metal junction allowing for dynamic heteroleptic aggregation with pyridine ligands proved to be successful in both solution and the solid state, as the combination of the concave $[Cu(phenAr_2)]^+$ with the corresponding bi-, tri-, and tetra-pyridyl compounds resulted in a series of supramolecular structures. Because of the highly dynamic and thermochemically weak copper(I)−pyridine interaction in solution, the resulting structures still pose a challenge to our present arsenal of analytical tools thus requiring the improvement of solution state characterization, in particular since aggregation in solution and the solid state in the present examples sometimes led to different structures.

Unlike the bidentate ligands 2,2-bipyridine or 1,10-phenanthroline, monodentate pyridyl ligands at the copper(I) center form a $N(py)-Cu^+-N(py)$ coordination angle ranging from 101.2 to 116.2°. This provides the desired increased flexibility useful for the design of highly complicated nanostructures and possibly lower barriers for dynamic repair. Work is in progress to demonstrate the ample usefulness of this concept.

Table 1. Summary of Crystallographic Data for Complexes **2**, **3n**, **4**, and **5**

	2	**3n**	**4**	**5**
formula	$C_{44}H_{36}Cl_2CuF_6N_4P$	$C_{432}H_{340}C_{l44}Cu_6F_{36}N_{24}P_6$	$C_{124}H_{96}Cl_8Cu_3F_{12}N_{12}P_2$	$C_{125}H_{98}Cl_{11}Cu_2F_{12}\ N_8P_2$
Fw	900.18	8678.14	2518.29	2519.08
Space group	$I4_1/acd$	$P2_1/n$	$P2_1/c$	$R\bar{3}$
a/Å	24.789(4)	23.226(9)	14.248(3)	26.457(11)
b/Å	24.789(4)	29.228(11)	16.735(3)	26.457(11)
c/Å	27.611(6)	64.59(3)	25.463(5)	102.846(8)
β/deg	90.00	97.852(18)	100.13(3)	90.00
V/Å^3	16967(5)	43438(30)	5977(2)	62345(37)
Z	16	4	2	18
D_{calc} (g cm^{-3})	1.410	1.327	1.399	1.208
R_1 [$I > 2\sigma(I)$]	0.0528	0.1501	0.1205	0.0709
wR_2 [$I > 2\sigma(I)$]	0.0999	0.1990	0.2994	0.1748

Experimental Part

All commercial reagents were used without further purification. The purification and drying of the solvents was accomplished according to standard methods. Thin-layer chromatography was performed using thin-layer chromatography plates (Merck, Silica Gel 60 F_{254}). Silica Gel 60 was equally used for column chromatography. Confirmation of the structures of all products was obtained by ^{1}H NMR and ^{13}C NMR spectroscopy (Bruker AC 200 and Avance 400 spectrometer, using the deuterated solvent as the lock and residual protiated solvent as the internal reference). ^{19}F and ^{31}P NMRs were measured without reference to see whether the PF_6^- ions were free ions or involved in host−guest complexes. The numbering of carbon atoms of the molecular formulas shown in the Experimental Section is only used for the assignment of the NMR signals and is not in accordance with the IUPAC nomenclature rules. Melting points were taken using an apparatus of Dr. Tottoli (Büchi) and are uncorrected. Electrospray mass spectra (ESI-MS) were recorded using a ThermoQuest LCQ Deca. The purity of all compounds was checked by thin-layer chromatography on SiO_2 (Merck, silica gel 60 F_{254}). Infrared spectra were recorded on a Perkin-Elmer 1750 FT-IR spectrometer.

Complex 1 (Solution State Characterization). Ligand **Phen1** (4.16 mg, 10.0 μmol) and [Cu(MeCN)$_4$]PF$_6$ (3.73 mg, 10.0 μmol) were dissolved in dichloromethane (0.50 mL) affording a slightly yellow solution. Then, 4,4′-bipyridine (**BP**, 1.56 mg, 10.0 μmol) was added resulting in an intensification of the yellow color. After removal of the solvents the solid residue was analyzed by FT-ICR MS, ^{1}H NMR, ^{13}C NMR, and elemental analysis without any further purification. The experimental evidence strongly supports the formation of [Cu(**Phen1**)(**BP**)]$_n^{n+}$ in solution. mp: > 300 °C; IR (KBr): = $\tilde{\nu}$ 3450, 2921, 1601, 1509, 1482, 1442, 1411, 1378, 1355, 1147, 1111, 840, 625, 558 cm^{-1}; ^{1}H NMR (400 MHz, CD_2Cl_2): δ = 8.72 (d, J = 8.3 Hz, 2H, 2-H), 8.19 (s, 2H, 1-H), 7.92 (d, J = 8.3 Hz, 2H, 3-H), 7.75 (d, J = 6.1 Hz, 4H, a-H), 7.39 (d, J = 6.1 Hz, 4H, b-H), 6.96 (s, 4H, 5-H), 2.32 (s, 6H, 6-H), 2.01 (s, 12H, 4-H); ^{13}C NMR (100 MHz, CD_2Cl_2): δ = 160.8, 151.0, 145.6, 144.0, 139.7, 139.5, 137.4, 136.2, 129.1, 128.4, 127.5, 127.2, 122.1, 21.2, 20.4; FT-ICR MS: calcd for [Cu(**Phen1**)(**BP**)]$^+$: m/z 635.2, found: m/z 635.2, calcd for [Cu$_2$(**Phen1**)$_2$(**BP**)(PF$_6$)]$^+$: m/z 1261.4, found: m/z 1261.4; Anal. Calcd for $C_{40}H_{36}CuF_6N_4P\cdot 0.5MeCN$ ([Cu(**Phen1**)(**BP**)(PF$_6$)]·0.5MeCN): C, 61.42; H, 4.71; N, 7.86; found C, 61.09; H, 4.46; N, 7.82.

Complex 2 (Solution and Solid State Characterization). Ligand **Phen2** (3.88 mg, 10.0 μmol) and [Cu(MeCN)$_4$]PF$_6$ (3.73 mg, 10.0 μmol) were dissolved in a mixture of dichloromethane and acetonitrile (0.50 mL, 19:1) to afford a slightly yellow solution. After addition of 4,4′-bipyridine (**BP**, 1.56 mg, 10.0 μmol), the yellow color of the solution intensified. After removal of the solvents, the solid residue was analyzed by FT-ICR MS, ^{1}H NMR, and ^{13}C NMR without any further purification. mp: > 300 °C; IR (KBr): = $\tilde{\nu}$ 3070, 1602, 1584, 1498, 1412, 1354, 1216, 1124, 1033, 867, 838, 779, 751, 557 cm^{-1}; ^{1}H NMR (400 MHz, CD_2Cl_2:CD_3CN (19:1)): δ = 8.67 (d, J = 8.2 Hz, 2H, 2-H), 8.21 (dd, J = 6.3 Hz, 1.6 Hz, 4H, a-H), 8.15 (s, 2H, 1-H), 7.86 (d, J = 8.2 Hz, 2H, 3-H), 7.45 (dd, J = 6.3 Hz, 1.6 Hz, 4H, b-H), 7.25 (t, J = 7.8 Hz, 2H, 6-H), 7.08 (d, J = 7.8 Hz, 4H, 5-H), 1.92 (s, 12H, 4-H); ^{13}C NMR (100 MHz, CD_2Cl_2:CD_3CN (19:1)): δ = 159.8, 150.7, 145.5, 143.9, 140.0, 138.4, 136.0, 129.3, 128.3, 127.8, 127.1, 126.8, 121.8, 20.0; FT-ICR MS: calcd for [Cu(**Phen2**)(**BP**)]$^+$: m/z 607.2, found: m/z 607.2, calcd for [Cu$_2$(**Phen2**)$_2$(**BP**)(PF$_6$)]$^+$: m/z 1203.3, found: m/z 1203.3, calcd for [Cu$_3$(**Phen2**)$_3$(**BP**)$_2$(PF$_6$)$_2$]$^+$: m/z 1958.4, found: m/z 1957.5; Anal. Calcd for $C_{38}H_{32}CuF_6N_4P\cdot C_6H_4Cl_2$ ([Cu(**Phen2**)(**BP**)(PF$_6$)]·1,2-dichlorobenzene): C, 58.71; H, 4.03; N, 6.22; found C, 58.38; H, 3.64; N, 6.30. Single crystals suitable for X-ray analysis were obtained by slow evaporation of acetonitrile from a 1,2-dichlorobenzene/acetonitrile (4:1) solution of **Phen2**, **BP**, and [Cu(MeCN)$_4$]PF$_6$ (1:1:1). For the solid state characterization, see the X-ray structural analysis.

Complex 3c (Solution State Characterization). 2,9-Dimesitylphenanthroline (**Phen1**, 4.16 mg, 10.0 μmol) and [Cu(MeCN)$_4$]PF$_6$ (3.73 mg, 10.0 μmol) were dissolved in dichloromethane (0.50 mL) affording a yellowish solution. Then, 1,3,5-trimethyl-2,4,6-tris(4-pyridinylethynyl)benzene[13] (**TP**, 2.82 mg, 6.66 μmol) was added whereupon the yellow color intensified. After removal of the solvent, the solid residue was analyzed by FT-ICR MS, ^{1}H NMR, ^{13}C NMR, DOSY, and elemental analysis without any further purification. mp: > 300 °C; IR (KBr): = $\tilde{\nu}$ 2919, 2207, 1606, 1492, 1481, 1379, 1357, 1214, 1148, 1111, 870, 841, 558 cm^{-1}; ^{1}H NMR (400 MHz, CD_2Cl_2): δ = 8.72 (d, J = 8.3 Hz, 12H, 2-H), 8.19 (s, 12H, 1-H), 7.93 (d, J = 8.3 Hz, 12H, 3-H), 7.65 (d, J = 6.3 Hz, 24H, a-H), 7.28 (d, J = 6.3 Hz, 24H, b-H), 6.97 (s, 24H, 5-H), 2.78 (s, 36H, c-H), 2.36 (s, 36H, 6-H) 2.01 (s, 72H, 4-H); ^{13}C NMR (100 MHz, CD_2Cl_2): δ = 160.8, 150.0, 144.9, 144.0, 139.8, 139.5, 137.4, 136.1, 132.5, 129.1, 128.4, 127.5, 127.2, 126.2, 121.0, 95.0, 92.5, 21.2, 20.6/20.4; FT-ICR MS: calcd for [Cu(**Phen1**)(**TP**)]$^+$: m/z 902.3, found: m/z 902.4; calcd for [Cu$_3$(**Phen1**)$_3$(**TP**)$_2$(PF$_6$)]$^{2+}$: m/z 1216.2, found: m/z 1215.9, calcd for [Cu$_2$(**Phen1**)$_2$(**TP**)(PF$_6$)]$^+$: m/z 1528.7, found: m/z 1528.5; calcd for [Cu$_4$(**Phen1**)$_4$(**TP**)$_3$(PF$_6$)$_2$]$^{2+}$: m/z 1740.4, found: m/z 1740.1; calcd for [Cu$_4$(**Phen1**)$_4$(**TP**)$_4$(PF$_6$)$_2$]$^{2+}$: m/z 1952.2, found: m/z 1951.7; calcd for [Cu$_5$(**Phen1**)$_5$(**TP**)$_3$(PF$_6$)$_3$]$^{2+}$: m/z 2053.0, found: m/z 2053.2; calcd for [Cu$_5$(**Phen1**)$_5$(**TP**)$_4$(PF$_6$)$_3$]$^{2+}$: m/z 2264.7, found: m/z 2264.8; calcd for [Cu$_6$(**Phen1**)$_6$(**TP**)$_4$(PF$_6$)$_4$]$^{2+}$: m/z 2577.2, found: m/z 2577.2; Anal. Calcd for $C_{300}H_{252}Cu_6F_{36}N_{24}P_6\cdot 2CH_2Cl_2$ ([Cu$_6$(**Phen1**)$_6$(**TP**)$_4$(PF$_6$)$_6$]·2CH$_2$Cl$_2$): C, 64.61; H, 4.60; N, 5.99; found C, 64.46; H, 4.24; N, 5.96.

Complex 3n. Single crystals suitable for X-ray analysis were obtained by slow evaporation of acetonitrile from a 1,2-dchlorobenzene/acetonitrile solution of **Phen1**, **TP**, and [Cu(MeCN)$_4$]PF$_6$ (6:4:6). For the solid state characterization, see the X-ray structural analysis.

Complex 4 (Solid State Characterization). 2,9-Dimesitylphenanthroline (**Phen1**, 3.88 mg, 10.0 μmol) and [Cu(MeCN)$_4$]PF$_6$

Table 2. Selected Bond Distances (Å) and Angles (deg) for **2**, **3n**, **4**, and **5**[a]

2			
Cu1−N1	2.043(3)	Cu1−N2	2.073(3)
N1−Cu1−N2	130.54(12)	N1−Cu1−N1$^{\#1}$	101.17(16)
N1−Cu1−N2$^{\#1}$	108.01(11)	N2−Cu1−N2$^{\#1}$	81.90(17)
3n			
Cu1−N12	1.970(8)	Cu1−N11	2.046(8)
Cu1−N24	2.068(8)	Cu1−N23	2.120(9)
Cu2−N4	1.988(8)	Cu2−N2	2.065(8)
Cu2−N17	2.068(8)	Cu2−N18	2.082(8)
Cu3−N3$^{\#2}$	1.966(8)	Cu3−N14	2.057(8)
Cu3−N1	2.075(8)	Cu3−N13	2.153(9)
Cu4−N8	1.980(8)	Cu4−N22	2.079(8)
Cu4−N10	2.083(8)	Cu4−N21	2.083(8)
Cu5−N7$^{\#3}$	1.995(8)	Cu5−N6	2.013(8)
Cu5−N16	2.063(8)	Cu5−N15	2.063(8)
Cu6−N9	1.953(9)	Cu6−N19	2.040(8)
Cu6−N5	2.059(8)	Cu6−N20	2.067(8)
N12−Cu1−N11	116.7(3)	N12−Cu1−N24	134.7(3)
N11−Cu1−N24	96.6(3)	N12−Cu1−N23	110.8(3)
N11−Cu1−N23	112.7(3)	N24−Cu1−N23	79.9(3)
N4−Cu2−N2	108.3(3)	N4−Cu2−N17	126.0(3)
N2−Cu2−N17	109.6(3)	N4−Cu2−N18	122.9(3)
N2−Cu2−N18	105.6(3)	N17−Cu2−N18	81.1(3)
N3$^{\#2}$−Cu3−N14	136.7(3)	N3$^{\#2}$−Cu3−N1	118.0(3)
N14−Cu3−N1	94.9(3)	N3$^{\#2}$−Cu3−N13	111.8(3)
N14−Cu3−N13	80.4(3)	N1−Cu3−N13	107.8(3)
N8−Cu4−N22	132.0(3)	N8−Cu4−N10	108.6(3)
N22−Cu4−N10	102.7(3)	N8−Cu4−N21	124.6(3)
N22−Cu4−N21	79.8(3)	N10−Cu4−N21	103.9(3)
N7$^{\#3}$−Cu5−N6	109.4(3)	N7$^{\#3}$−Cu5−N16	121.4(3)
N6−Cu5−N16	108.7(3)	N7$^{\#3}$−Cu5−N15	118.3(3)
N6−Cu5−N15	114.8(3)	N9−Cu6−N19	133.6(3)
N16−Cu5−N15	81.8(3)	N9−Cu6−N5	107.6(4)
N19−Cu6−N5	102.7(3)	N9−Cu6−N20	123.7(4)
N19−Cu6−N20	81.4(3)	N5−Cu6−N20	102.4(3)
4			
Cu1−N3	1.998(13)	Cu1−N1	2.050(11)
Cu1−N4$^{\#4}$	2.072(11)	Cu1−N2	2.124(13)
Cu2−N6	1.972(11)	Cu2−N5	2.010(10)
N3−Cu1−N1	134.5(5)	N3−Cu1−N4$^{\#4}$	104.5(5)
N1−Cu1−N4$^{\#4}$	104.5(5)	N3−Cu1−N2	126.0(5)
N1−Cu1−N2	79.4(5)	N4$^{\#4}$−Cu1−N2	103.3(5)
N6$^{\#5}$−Cu2−N5	89.2(4)	N6−Cu2−N5	90.8(4)
5			
Cu1−N3$^{\#6}$	1.977(5)	Cu1−N4$^{\#7}$	1.979(5)
Cu1−N1	2.070(5)	Cu1−N2	2.107(5)
Cu2−N8$^{\#8}$	1.962(4)	Cu2−N7$^{\#9}$	1.980(5)
Cu2−N5	2.091(4)	Cu2−N6	2.108(4)
N3$^{\#6}$−Cu1−N4$^{\#7}$	120.4(2)	N3$^{\#6}$−Cu1−N1	114.3(2)
N4$^{\#7}$−Cu1−N1	111.3(2)	N3$^{\#6}$−Cu1−N2	111.2(2)
N4$^{\#7}$−Cu1−N2	112.1(2)	N1−Cu1−N2	80.9(2)
N8$^{\#8}$−Cu2−N7$^{\#9}$	119.2(2)	N8$^{\#8}$−Cu2−N5	111.26(19)
N7$^{\#9}$−Cu2−N5	114.39(19)	N8$^{\#8}$−Cu2−N6	116.44(18)
N7$^{\#9}$−Cu2−N6	108.6(2)	N5−Cu2−N6	80.89(18)

[a] Symmetry transformations used to generate equivalent atoms: (#1) $-y$, $x+5/2$, $z+5/4$; (#2) $-x+4$, $y-1/2$, $-z+1$; (#3) x, $y+1$, z; (#4) x, $-y+3/2$, $z+3/2$; (#5) $-x+2$, $-y+1$, $-z-1$; (#6) $y+2/3$, $-x+y+1/3$, $-z+1/3$; (#7) $-y$, $x-y-1$, z; (#8) $-y$, $x-y$, z; (#9) y, $-x+y$, $-z$.

(5.59 mg, 15.0 μmol) were dissolved in a mixture of 1,2-dichlorobenzene and acetonitrile (10.0 mL, 9:1) to afford a slightly yellow solution. Then, *meso*-tetra(4-pyridyl)porphyrin (**TPP**, 3.09 mg, 5.00 μmol) was added, and the mixture was heated to reflux for 30 min. The solution was put aside, and after slow evaporation of acetonitrile, dark red single crystals were obtained. mp: >300 °C; IR (KBr): = $\tilde{\nu}$ 3438, 2916, 1601, 1543, 1481, 1456, 1415, 1378, 1349, 1325, 1304, 1208, 1137, 1125, 1084, 1061, 1032, 999, 893, 855, 798, 757, 716, 625, 494 cm^{-1}. For the solid state characterization, see the X-ray structural analysis. Because of the low solubility of Cu-**TPP** and Zn-**TPP**, free base porphyrin of **TPP** was used. By copper insertion **TPP** was completely converted to Cu-**TPP**.

Complex 5 (Solution State Characterization). Phen3 (5.99 mg, 10.0 μmol) and [Cu(MeCN)$_4$]PF$_6$ (3.73 mg, 10.0 μmol) were dissolved in dichloromethane (0.50 mL) to afford yellow solution. After removal of solvent the solid residue was analyzed by FT-ICR MS, ^{1}H NMR, ^{13}C NMR, DOSY, and elemental analysis without any further purification. mp: >300 °C; IR (KBr): = $\tilde{\nu}$ 2964, 1607, 1585, 1504, 1416, 1385, 1356, 1262, 1098, 1019, 876, 843, 804, 577, 558 cm^{-1}; ^{1}H NMR (400 MHz, acetone-d6): δ = 9.01 (d, J = 8.3 Hz, 12H, 2-H), 8.46 (s, 12H, 1-H), 8.36−8.39 (m, 12H, 7$_a$−H), 8.18−8.20 (m, 12H, 7$_b$−H), 8.01(dd, J = 8.3 and 2.0 Hz, 12H, 3-H), 7.29−7.31 (m, 12H, 6$_a$−H), 7.12−7.21 (m, 12H, 6$_b$−H), 1.79 (s, 72H, 4-H) 1.61 (s, 72H, 5-H); ^{13}C NMR (100 MHz, acetone-d6): δ = 161.1, 153.3, 153.1, 153.4, 149.9, 145.1, 141.9, 140.0, 139.2, 132.9, 131.4, 129.9, 128.3, 126.9, 126.6, 18.8, 18.7; ESI-MS: calcd for [M−6(PF$_6$)]$^{6+}$: m/z 662.3, found: m/z 662.6, calcd for [M−5(PF$_6$)]$^{5+}$: m/z 823.8, found: m/z 823.6, calcd for [M−4(PF$_6$)]$^{4+}$: m/z 1066.0, found: m/z 1066.8, calcd for [M−3(PF$_6$)]$^{3+}$: m/z 1469.6, found: m/z 1469.1; Anal. Calcd for $C_{252}H_{228}Cu_6F_{36}N_{24}P_6\cdot 6CH_2Cl_2\cdot 2CH_3CN$ ([Cu$_6$(**Phen3**)$_6$(PF$_6$)$_6$]·6CH$_2$Cl$_2$·2CH$_3$CN): C, 57.89; H, 4.56; N, 6.70; found C, 57.55; H, 4.62; N, 6.74. Single crystals suitable for X-ray analysis were obtained by slow vapor diffusion of diethyl ether into a 1,2-dichlorobenzene solution of **Phen3** and [Cu(MeCN)$_4$]PF$_6$ (1:1). For the solid state characterization, see the X-ray structural analysis.

X-ray Data Collection and Structure Determinations. X-ray single-crystal diffraction data for complexes **2**, **4**, and **5** were collected on a STOE IPDS one-circle image plate diffractometer and for **3n** on a SIEMENS SMART diffractometer. The structures were solved using SHELXS-97 and refined by full-matrix least-squares analysis.[20] The hydrogen atoms were generated theoretically onto the specific atoms and refined isotropically with fixed thermal factors. The non-H atoms in **2**, **4**, and **5** were refined with anisotropic thermal parameters. There are disordered solvent molecules and anions in the crystal lattice of compound **5**, whose contribution to the structural data was removed by the SQUEEZE function.[21] In **3n** the non-H atoms of solvent molecules are refined isotropically because of low quality of the sample. The crystal parameters, data collection, and refinement results for compounds **2**, **3n**, **4**, and **5** are summarized in Table 1. Selected bond lengths and angles are listed in Table 2. Further details are provided in the Supporting Information.

Acknowledgment. We are grateful to the Deutsche Forschungsgemeinschaft and the University of Siegen for continued support and are deeply indebted to the Alexander von Humboldt Stiftung for a AvH stipend for J.F. This manuscript is dedicated to Prof. Dr. H.-D. Lutz on the occasion of his 75th birthday.

Supporting Information Available: Experimental details, mass spectra, NMR data, and crystal data. This material is available free of charge via the Internet at http://pubs.acs.org.

(20) (a) Sheldrick, G. M. *SHELXS97: Program for Crystal Structure Determination*; University of Göttingen: Göttingen, Germany, 1997. (b) Sheldrick, G. M. *SHELXL97: Program for Crystal Structural Refinement*; University of Göttingen: Göttingen, Germany, 1997.

(21) (a) Spek, A. L. *Acta Crystallogr.* **1990**, *A46*, C34. (b) Spek, A. L. *PLATON, A Multipurpose Crystallographic Tool*; Ultrecht University: Ultrecht, The Netherlands, 2006.